PNAS RESEARCH ARTICLE | IMMUNOLOGY AND INFLAMMATION

NRF2 is a spatiotemporal metabolic hub essential for the polyfunctionality of Th2 cells

Garam Choi[a,1], Hye-Yeon Ju[b,1], Jahyun Bok[a,1], Jungseo Choi[a], Jae Woo Shin[c], Hansol Oh[d], Yeojin Jeon[a], Jiyeon Kim[a], Daehong Kim[a], Heesu Moon[a], Jeong-Eun Lee[a], Young-Sam Keum[e], You-Me Kim[f], Hye Young Kim[c], Sung Ho Park[d,2], Mi-Ryung Han[b,2], and Yeonseok Chung[a,2]

Affiliations are included on p. 12.

Edited by Casey Weaver, Department of Pathology, The University of Alabama, Birmingham, AL; received November 14, 2023; accepted May 20, 2024

Upon encountering allergens, CD4$^+$ T cells differentiate into IL-4-producing Th2 cells in lymph nodes, which later transform into polyfunctional Th2 cells producing IL-5 and IL-13 in inflamed tissues. However, the precise mechanism underlying their polyfunctionality remains elusive. In this study, we elucidate the pivotal role of NRF2 in polyfunctional Th2 cells in murine models of allergic asthma and in human Th2 cells. We found that an increase in reactive oxygen species (ROS) in immune cells infiltrating the lungs is necessary for the development of eosinophilic asthma and polyfunctional Th2 cells in vivo. Deletion of the ROS sensor NRF2 specifically in T cells, but not in dendritic cells, significantly abolished eosinophilia and polyfunctional Th2 cells in the airway. Mechanistically, NRF2 intrinsic to T cells is essential for inducing optimal oxidative phosphorylation and glycolysis capacity, thereby driving Th2 cell polyfunctionality independently of IL-33, partially by inducing PPARγ. Treatment with an NRF2 inhibitor leads to a substantial decrease in polyfunctional Th2 cells and subsequent eosinophilia in mice and a reduction in the production of Th2 cytokines from peripheral blood mononuclear cells in asthmatic patients. These findings highlight the critical role of Nrf2 as a spatial and temporal metabolic hub that is essential for polyfunctional Th2 cells, suggesting potential therapeutic implications for allergic diseases.

NRF2 | metabolic fitness | Th2 cell | OXPHOS | PPARγ

Unnecessarily aggressive helper T cell immunity is a main cause of chronic immune disorders such as autoimmune or allergic diseases (1, 2). In particular, polyfunctional T cells that can perform multiple functions contribute to the pathogenesis of immune disorders by producing multiple cytokines. For instance, polyfunctional Th17 cells producing high levels of IL-17, IFNγ, and TNFα have been found to contribute to joint inflammation and damage in arthritis (3, 4). In cases of allergic diseases, polyfunctional Th2 cells producing a combination of type 2 cytokines including IL-4, IL-5, and IL-13 are found in the inflamed tissues (5). Polyfunctional T cells are typically generated in response to repeated exposure to antigens in the nonlymphoid tissues, as opposed to initially differentiated effector T cells in the lymph nodes, which typically have less polyfunctionality (6).

The mechanism by which initial effector T cells acquire polyfunctionality remains incompletely understood. One possible mechanism is the cytokine gene cluster that contains several genes encoding cytokines and chemokines. For instance, genes encoding IL-4, IL-5, and IL-13 are clustered within a 150 kb region in the same chromosome, termed "Th2 cytokine gene cluster" (7), suggesting that these type 2 cytokine genes might be regulated in a coordinated manner. Notably, type 2 immune cells including Th2 cells and type 2 innate lymphoid cells (ILC2s) show divergent expression of these cytokines depending on the types of cells and tissues during allergic responses. Th2 cells initially primed in the draining lymph nodes express IL-4 with little IL-5 and IL-13, while Th2 cells in the allergic lungs and skins coexpress IL-5 and/or IL-13 in addition to IL-4 (8–10). Thus, Th2 cells need to receive cues in the nonlymphoid tissues, such as lung and skin, to terminally differentiate into IL-5- and/or IL-13-producing polyfunctional Th2 cells in allergic diseases (2, 11). Tissue-derived alarmin cytokines such as IL-33 have been proposed to be responsible for the differentiation of polyfunctional Th2 cells in the tissues (9). By contrast, several studies have reported that ST2-deficiency failed to reduce, but rather enhance, the production of type 2 cytokines from Th2 cells in animal models (12, 13), suggesting that IL-33 may not be involved in the differentiation of polyfunctional Th2 cells. In this regard, it has been shown that ST2 expression is selectively increased on memory Th2 cells, and thus IL-33 induces the production of IL-5 from memory Th2 cells, but not from effector Th2 cells (14). Considering these findings, it is feasible to surmise that tissue-specific or cell-intrinsic factors other than alarmins

Significance

Initially, differentiated Th2 cells are capable of producing IL-4. These cells then migrate into inflamed tissues, where they further differentiate into polyfunctional Th2 cells capable of producing multiple cytokines including IL-5, IL-9, and IL-13. The molecular mechanism by which initial Th2 cells acquire polyfunctionality in tissues remains unclear. We demonstrate that cell-intrinsic NRF2, a transcription factor responsible for antioxidant responses, is essential for the differentiation of polyfunctional Th2 cells in allergic asthma. Mechanistically, NRF2 drives optimal oxidative phosphorylation (OXPHOS) and glycolysis in Th2 cells, partially through PPARγ, to establish polyfunctionality in tissue-infiltrating Th2 cells. Since NRF2 also regulates polyfunctionality of human Th2 cells, our findings accentuate the possibility of targeting NRF2–OXPHOS/glycolysis pathway to treat Th2 cell-related diseases in humans.

The authors declare no competing interest.

This article is a PNAS Direct Submission.

[1]G.C., H.-Y.J., and J.B. contributed equally to this work.

[2]To whom correspondence may be addressed. Email: parksu@unist.ac.kr, genetic0309@inu.ac.kr, or yeonseok@snu.ac.kr.

This article contains supporting information online at https://www.pnas.org/lookup/suppl/doi:10.1073/pnas.2319994121/-/DCSupplemental.

Published July 3, 2024.

contribute to the polyfunctional differentiation of Th2 cells during allergic inflammation.

Inhalation of foreign matters such as xenobiotics often triggers oxidative stress in the lung, and cells receiving oxidative stress quickly activate an antioxidant program. The increase of oxidative stress leads to dissociation of NRF2 from Keap1 in the cytosol and its translocation into nucleus where it initiates the transcription of genes encoding antioxidant molecules. Similar to xenobiotics, allergens, such as those derived from fungal, pollen, and house dust mite (HDM), have been shown to trigger oxidative stress (15).

In the present study, we demonstrate that T cell-intrinsic NRF2 activation is essential for optimal oxidative phosphorylation (OXPHOS) and glycolysis capacity in Th2 cells, leading to the production of multiple type 2 cytokines in murine and human Th2 cells. Thus, NRF2 serves as a spatiotemporal metabolic hub that induces polyfunctionality in Th2 cells in vivo.

Results

Elevation of Intracellular ROS Is Required for the Induction of Allergic Asthma. To investigate the mechanisms through which initial Th2 cells acquire polyfunctionality in vivo, we employed animal models of allergic asthma induced by intranasal challenges with fungal protease from *Aspergillus oryzae* plus ovalbumin (PAO/Ova) or HDM extract to induce Th2-mediated allergic asthma (Fig. 1*A* and *SI Appendix*, Fig. S1*A*) (16, 17). Allergen-primed initial Th2 cells predominantly produce IL-4 in the draining lymph nodes, but they additionally produce IL-5 and/or IL-13 after migrating to the lung (18). Our hypothesis was that if a cell-intrinsic factor plays a critical role in the polyfunctional program of Th2 cells, its levels would be significantly altered in the lung-infiltrating Th2 cells compared to those in the draining lymph nodes. In the mediastinal lymph nodes (medLNs), most types of immune cells, with the exception of $CD11b^+$ cells $CD44^{hi}CD8^+$ T cells, exhibited comparable levels of intracellular ROS between PAO/Ova-challenged and unchallenged mice, as indicated by DCFDA staining (Fig. 1*B* and *SI Appendix*, Fig. S1 *B* and *C*). In contrast, within the lungs of challenged mice, all types of immune cells displayed significantly higher levels of intracellular ROS compared to those in the lungs of unchallenged mice. This increase in intracellular ROS was evident in both $CD44^{lo}$ and $CD44^{hi}$ populations of $CD4^+$ T and $CD8^+$ T cells. The levels of ROS were also elevated in $CD45.2^-$ cells within the challenged lungs. Consequently, in the challenged mice, all types of immune cells within the lungs exhibited significantly higher intracellular ROS levels when compared to the medLNs (Fig. 1*C*). We also used an HDM-induced asthma model and observed a similar increase in the levels of intracellular ROS in all types of immune cells tested in the lungs relative to the medLNs (*SI Appendix*, Fig. S1 *A*, *D*, and *E*). Thus, intranasal allergens trigger an increase in intracellular ROS in the immune cells infiltrated in the lung, but not in the medLNs, regardless of their activation status.

Given that signaling through the T cell receptor is known to trigger ROS in activated T cells (19, 20), it was unexpected to observe that $CD44^{lo}$ T cells in the lungs of asthmatic mice had similar levels of ROS to $CD44^{hi}$ T cells. To determine whether antigen-specific activation affects the induction of ROS in $CD4^+$ T cells, we adoptively transferred naive OT-II T cells into congenic mice prior to intranasal administration of PAO/Ova (Fig. 1*D*). As depicted in Fig. 1*E*, regardless of the level of CD44 expression, both recipient (polyclonal) and donor (monoclonal and antigen-specific) $CD4^+$ T cells in the lungs had higher levels of intracellular ROS than those in the medLN. Moreover, there were little variations in ROS levels between recipient and donor $CD4^+$ T cells, in both $CD44^{hi}$ and $CD44^{lo}$ populations, indicating that the increase in ROS in the lung-infiltrated T cells is independent of antigen-specific activation.

To investigate the impact of increased intracellular ROS on the development of allergic asthma, we administered N-acetyl cysteine (NAC) to deplete ROS during the induction of allergic asthma (Fig. 1*F*). NAC is a potent antioxidant by itself as well as after conversion into GSH (21–24). Treatment with NAC resulted in a significant reduction in the number of inflammatory cells in the bronchoalveolar lavage (BAL), primarily attributed to a decrease in eosinophil count (Fig. 1 *G* and *H*). Furthermore, NAC treatment led to a notable decrease in the absolute number of $IL\text{-}5^+$ and/or $IL\text{-}13^+$ Th2 cells (Fig. 1*I*). These findings demonstrate that during allergic asthma, there is a substantial induction of intracellular ROS in lung-infiltrated immune cells regardless of their cell type or activation status. Moreover, the blockade of ROS significantly attenuates eosinophilia and polyclonal Th2 cell responses in the airway.

T Cell-Intrinsic NRF2 Is Required for the Differentiation of Polyfunctional Th2 Cells In Vivo. ROS activates NRF2 by releasing it from Keap1, facilitating the translocation of NRF2 to the nucleus where it induces the expression of various antioxidant enzymes and cytoprotective proteins (25). We observed that transcript levels of *Nfe2l2*, the gene encoding NRF2, as well as its target genes *Nqo1, Hmox1, Gclc,* and *Gclm* were higher in the lung compared to the medLNs. Furthermore, these transcript levels were up-regulated following intranasal allergen challenges (*SI Appendix*, Fig. S1*F*). We also found significantly higher levels of *NQO1*, *GCLC*, and *GCLM* in the lungs of severe asthmatic patients compared to healthy individuals (*SI Appendix*, Fig. S1*G*), suggesting the potential involvement of NRF2 in allergic asthma in vivo. Therefore, we hypothesized that allergenic challenges induce an increase in ROS and activate NRF2 in immune cells that infiltrate the lungs during allergic asthma. To test this hypothesis, we induced allergic asthma in mice through intranasal PAO/Ova challenges and treated them with either an NRF2 inhibitor (ML385) or DMSO as a vehicle control (Fig. 1*J*). Similar to NAC treatment, NRF2 inhibitor treatment led to a significant reduction in eosinophil frequency in the BAL fluid, as well as a decrease in inflammatory cell infiltration and the frequency of mucus-containing goblet cells (Fig. 1 *K*–*M*). The levels of IL-5 and IL-13 in the BAL fluid, as well as the frequency of IL-5- and IL-13-producers among $CD4^+$ T cells, were remarkably reduced by ML385 treatment (Fig. 1 *N* and *O*). In addition to Th2 cells, ILC2s have been implicated in contributing to type 2 inflammation in the lung (26, 27). To determine whether NRF2 also influences the induction and expansion of ILC2, we intranasally challenged Rag1-deficient mice with papain together with ML385 or vehicle (*SI Appendix*, Fig. S1*H*). Unlike Th2 cells, however, we observed little change in the frequency of $IL\text{-}5^+IL\text{-}13^+$ ILC2s and $CD206^+$ macrophages following ML385 treatment (*SI Appendix*, Fig. S1 *I* and *J*).

To gain insights into the mechanism by which NRF2 contributes to polyfunctional Th2 cell, we first focused on dendritic cells as they play a crucial role in the initial differentiation of helper T cells. To study this, we generated mutant mice lacking *Nfe2l2* in $CD11c^+$ cells (referred to as $CD11c^{\Delta NRF2}$). Surprisingly, we observed little differences in the numbers of eosinophil and Th2 cell in the BAL and the lung between $CD11c^{\Delta NRF2}$ and littermate control (*SI Appendix*, Fig. S2 *A* and *B*), ruling out any involvement of NRF2 in dendritic cells in the development of allergic asthma.

We next determined the role of NRF2 in $CD4^+$ T cells by generating T cell–specific *Nfe2l2* deficient mice (referred to as

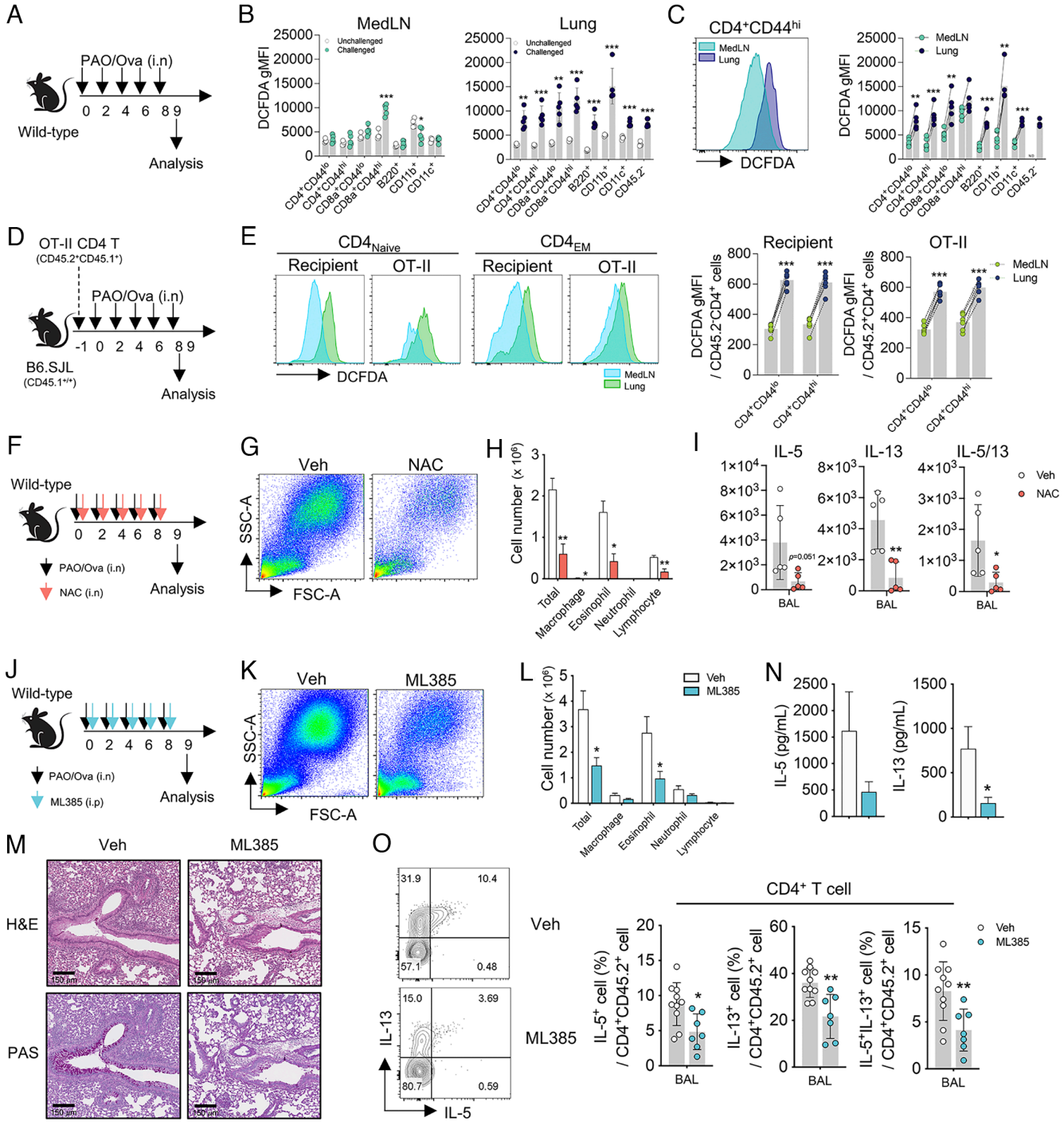

Fig. 1. Increase of ROS and subsequent activation of NRF2 in lung-infiltrating cells are required for polyfunctional Th2 cells and eosinophilia in allergic asthma. (*A–C*) C57BL/6 mice were intranasally challenged with PAO/Ova to induce allergic asthma. Schematic representation (*A*) and the levels of ROS in the indicated cell types in the medLN and the lung (*B* and *C*). (*D* and *E*) Recipient (CD45.1$^{+/+}$) of OT-II T cells (CD45.2$^{+/+}$) were challenged with intranasal PAO/Ova. Schematic representation (*D*), and the levels of ROS in the indicated T cell population (*E*). (*F–I*) C57BL/6 mice were subjected to PAO/Ova-induced allergic asthma and additionally given intranasal NAC or vehicle. Schematic representation (*F*) and representative FACS plot of BAL fluid cells (*G*). Differential cell counts (*H*) and Absolute numbers of IL-5$^+$ (*Left*), IL-13$^+$ (*Middle*), or IL-5$^+$IL-13$^+$ (*Right*) cells (*I*) in the BAL fluid. (*J–O*) C57BL/6 mice were subjected to PAO/Ova-induced allergic asthma and additionally given intraperitoneal ML385 or vehicle. Schematic representation (*J*) and representative FSC/SSC FACS plots (*K*), differential cell counts (*L*), or the levels of IL-5 and IL-13 (*M*) in the BAL fluid. Hematoxylin and eosin (H&E) and periodic acid–Schiff (PAS) staining of the lung (*N*) or representative contour plots and quantification of IL-5- and/or IL-13-expressing cells in CD45.2$^+$CD4$^+$ T cells in the BAL fluid (*O*). Data are representative of three independent experiments. Quantification plots show the means ± SD (*B*, *I*, and *O*) or ±SEM (*H*, *L*, and *M*); **P* < 0.05, ***P* < 0.01, and ****P* < 0.001. Statistical analysis: unpaired Student's *t* test (*B*, *H*, and *I*), paired Student's *t* test (*C* and *E*).

CD4$^{\Delta NRF2}$) (*SI Appendix*, Fig. S2 *C* and *D*). CD4$^{\Delta NRF2}$ mice displayed normal T cell development in the thymus, and NRF2-deficient naive CD4$^+$ T cells showed intact proliferation in response to plate-bound anti-CD3 (*SI Appendix*, Fig. S2 *E* and *F*). Intriguingly, when challenged with intranasal allergens, CD4$^{\Delta NRF2}$ mice had a significant reduction of granulocytes, mainly eosinophils, in the BAL fluid relative to littermate control (Fig. 2 *A* and *B*). Moreover, we observed a significant reduction in the inflammatory cells as well as mucus-containing goblet cells in the lung in the former (Fig. 2*C*). Flow cytometric analyses revealed a drastic reduction in the frequencies of IL-5- and IL-13-producing CD4$^+$ T cells, while the frequencies of Th1,

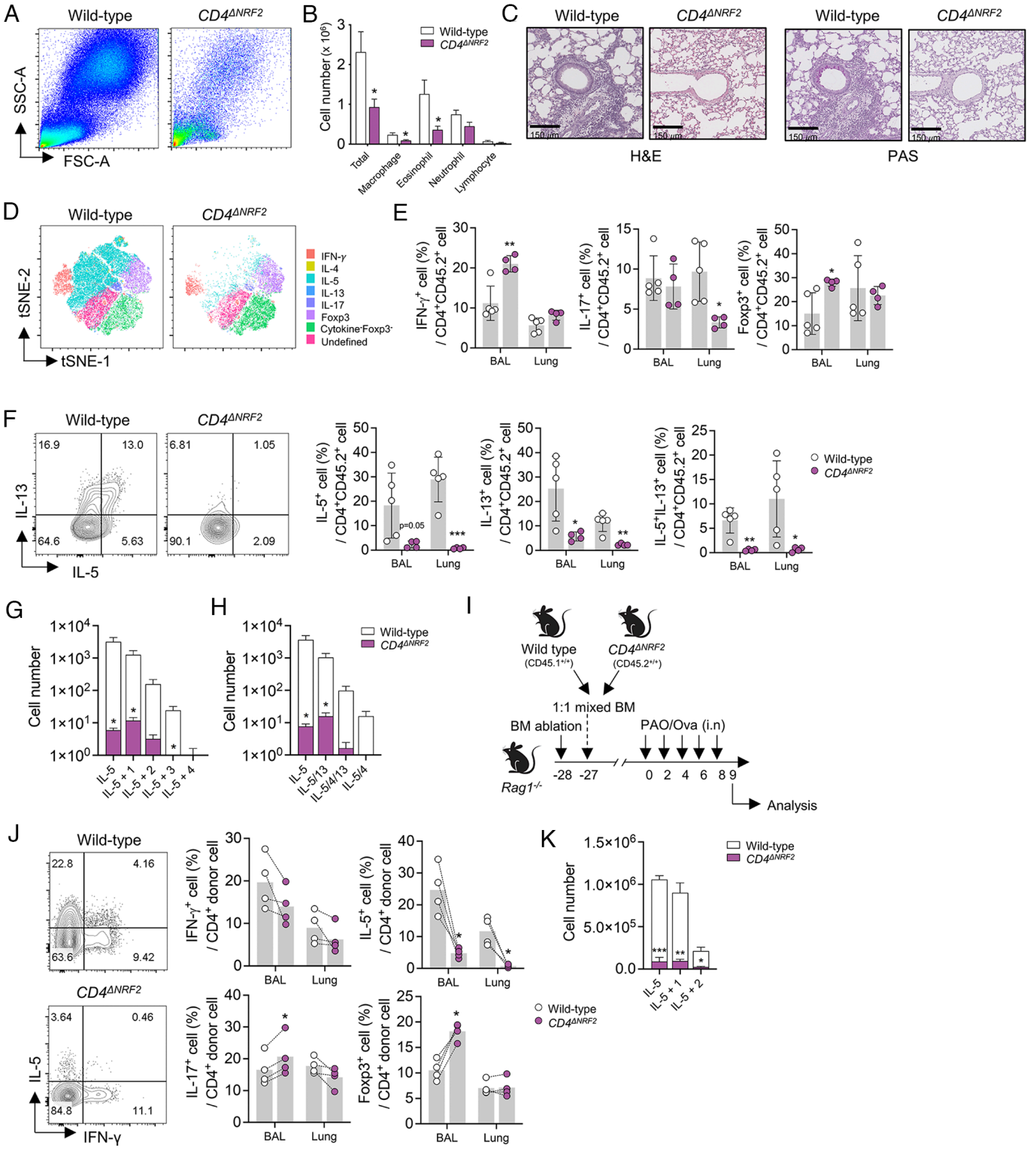

Fig. 2. T cell–intrinsic NRF2 is essential for the differentiation of polyfunctional Th2 cells in vivo. (*A–H*) T cell–specific NRF2-deficient mice (*CD4*$^{\Delta NRF2}$) and littermate control mice wild-type (WT) were subjected to PAO/Ova-induced allergic asthma. Representative FSC/SSC FACS plot (*A*) and differential cell counts (*B*) of the cells in BAL fluid. (*C*) H&E and PAS staining of the lung from indicated mice. (*D*) tSNE visualization of intracellular staining of CD4$^+$ T cells in the BAL fluid of indicated mice. (*E*) Quantification of IFN-γ-, IL-17-, or Foxp3-expressing cells in CD45.2$^+$CD4$^+$ cells from the BAL fluid and the lungs. (*F*) Representative contour plots and quantification of IL-5- and/or IL-13-expressing cells in CD45.2$^+$CD4$^+$ cells from the BAL fluid. (*G*) Numbers of IL-5$^+$CD4$^+$ T cells expressing additional cytokines. (*H*) Numbers of Th2 cells expressing the indicated type 2 cytokines. (*I–K*) BM chimeric mice were generated by adoptive transfer of 1:1 mixture of WT and *CD4*$^{\Delta NRF2}$ BM into irradiated *Rag1*$^{-/-}$ mice. After the reconstitution period, the chimeras were subjected to PAO/Ova-induced allergic asthma. Schematic representation of mixed bone marrow chimera study (*I*) and representative plots and quantification of CD4$^+$ T cells producing indicated cytokines (*J*). Numbers of IL-5$^+$CD4$^+$ T cells expressing additional cytokines (*K*). Data are representative of three independent experiments. Quantification plots show the means ± SEM (*B*, *G*, *H*, and *K*) or ±SD (*E* and *F*); **P* < 0.05, ***P* < 0.01, and ****P* < 0.001. Statistical analysis: unpaired Student's *t* test *B* and *E–H*), paired Student's *t* test (*J* and *K*).

Th17, and Treg cells remained relatively comparable in the BAL fluid of $CD4^{\Delta NRF2}$ mice (Fig. 2 *D*–*F*). In particular, the numbers of polyfunctional Th2 cells, producing 2 or more type 2 cytokines, were all significantly diminished (over 90 % reduction) in the BAL fluid of the $CD4^{\Delta NRF2}$ mice (Fig. 2 *F*–*H*). We also observed decreased levels of *Cxcl1*, *Ccl11*, *Muc5ac*, and *Clca3* in the lungs of $CD4^{\Delta NRF2}$ mice compared with control mice (*SI Appendix*, Fig. S2*G*). Consistently, we also observed a drastic reduction in the numbers of eosinophils and polyfunctional Th2 cells in the BAL fluid of $CD4^{\Delta NRF2}$ mice in the HDM-induced asthma model (*SI Appendix*, Fig. S2 *H* and *I*). Since *Cd4-cre* system also deletes loxp-flanked target genes in $Foxp3^+$ Treg cells, we asked whether the reduced polyfunctional Th2 cells in the $CD4^{\Delta NRF2}$ mice were due to NRF2-deficiency in Treg cells by generating Treg-specific NRF2-deficient (referred to as $Foxp3^{\Delta NRF2}$) mice. Unlike $CD4^{\Delta NRF2}$ mice, however, the numbers of eosinophils, Th2 cells, and $Foxp3^+$ Treg cells in the BAL fluid were all comparable between $Foxp3^{\Delta NRF2}$ mice and control littermates ($Nfe2l2^{fl/fl}$) (*SI Appendix*, Fig. S2 *J* and *K*), indicating little role of NRF2 in $Foxp3^+$ Treg cells in regulating allergic lung inflammation.

The defective Th2 cell responses observed in $CD4^{\Delta NRF2}$ mice, coupled with intact Th2 cell responses in $CD11c^{\Delta NRF2}$ and $Foxp3^{\Delta NRF2}$ mice, demonstrate that NRF2 expression in conventional T cells is essential for the development of polyfunctional Th2 cells and eosinophilic inflammation. To investigate whether NRF2 mediates the differentiation of polyfunctional Th2 cells in a cell-intrinsic manner, we generated mixed bone marrow chimeras by transferring 1:1 bone marrow mixture of $CD4^{\Delta NRF2}$ and congenic WT mice into irradiated $Rag1^{-/-}$ mice (Fig. 2*I*). We observed an almost complete reduction of IL-5-producers among the NRF2-deficient $CD4^+$ T cells compared to the $CD45.1^+$ WT cells in the same mice (Fig. 2*J*). We also observed a trend toward reduced Th1 cells in the NRF2-deficient $CD4^+$ T cell population, while the frequencies of Th17 and Treg cells were increased, in the BAL, but not in the lungs. Moreover, the number of Th2 cells producing multiple type 2 cytokines was also significantly diminished in the former population (Fig. 2*K*). Collectively, these results provide strong evidence for an indispensable role of T cell-intrinsic NRF2 in the differentiation of polyfunctional Th2 cells in vivo.

NRF2 Promotes the Differentiation of Polyfunctional Th2 Cells in the Lung Independently of IL-33. To further interrogate the mechanism by which NRF2 induces Th2 cell responses in vivo, we determined whether NRF2 is necessary for the differentiation of naive T cells into initial Th2 cell capable of producing IL-4 in the medLNs during allergic asthma. We generated $Il4^{GFP}CD4^{\Delta NRF2}$ mice and $Il4^{GFP}Nfe2l2^{fl/fl}$mice by crossing IL-4-eGFP reporter (4get) mice with $CD4^{\Delta NRF2}$ mice or $Nfe2l2^{fl/fl}$, respectively. Upon challenging these mice with intranasal allergens, both $Il4^{GFP}CD4^{\Delta NRF2}$ mice and $Il4^{GFP}Nfe2l2^{fl/fl}$mice exhibited similar frequencies of IL-4-GFP^+ among $CD4^+$ T cells in the medLNs; however, we observed a significant reduction in the frequency of IL-4-GFP^+ among $CD4^+$ T cells in the lungs of $Il4^{GFP}CD4^{\Delta NRF2}$ mice (Fig. 3 *A* and *B*). We conducted an analysis on Tfh cells since Tfh cells constitute a significant portion of IL-4^+ cells present in the lymph nodes, in addition to Th2 cells (28). Among those IL-4^+ cells in the medLNs, the frequencies of $CXCR5^+PD1^+$ Tfh cells and Th2 cells appeared to be comparable between $CD4^{\Delta NRF2}$ and WT mice (*SI Appendix*, Fig. S3 *A* and *B*). The frequencies of $CD4^+$ T cells among total lymphocytes in the lungs and in the medLNs were also comparable between the two groups (*SI Appendix*, Fig. S3*C*). Thus, NRF2 does not likely regulate the generation of IL-4-producing $CD4^+$ T cells in the medLNs nor the recruitment of $CD4^+$ T cells into the lung but is required for the terminal differentiation of initially primed Th2 cells within the lung. To directly address this point, we generated ERT2-cre×$Nfe2l2^{fl/fl}$ (cre-$ERT2^{\Delta NRF2}$) mice, in which *Nfe2l2* can be deleted by tamoxifen treatment. Naive $CD4^+$ T cells from cre-$ERT2^{\Delta NRF2}$ mice were differentiated into Th2 cells and then either treated with 4-hydroxytamoxifen (4-OHT) or left untreated. Subsequently, the Th2 cells were restimulated with IL-33 in the presence of IL-2 (Fig. 3*C*). Notably, deletion of *Nfe2l2* in in vitro-differentiated Th2 significantly impaired the production of IL-5 and IL-13 upon restimulation (Fig. 3 *D* and *E*). Additionally, we employed ML385, an NRF2 inhibitor, and found that it also inhibited the production of these type 2 cytokines from Th2 cells after restimulation with IL-25 or IL-33 (*SI Appendix*, Fig. S4 *A* and *B*). Treatment with ML385 minimally affected the differentiation of Th1, Th17, and Treg cells from naive $CD4^+$ T cells in vitro (*SI Appendix*, Fig. S4 *C* and *D*). These results highlight the essential role of NRF2 for the differentiation of initial Th2 cells into polyfunctional Th2 cells.

Studies using $Il33^{-/-}$ or $Il1rl1^{-/-}$ mice revealed a role for IL-33 in amplifying type 2 inflammation in vivo by acting on ILC2 and effector/memory Th2 cell (14, 29, 30), raising a possible involvement of IL-33/ST2 in NRF2-mediated differentiation of polyfunctional Th2 cells. To further investigate whether NRF2 promotes differentiation of polyfunctional Th2 cells via IL-33/ST2 pathway, we examined the expression of ST2 on IL-4-GFP^+ T cells in the lung of $Il4^{GFP}CD4^{\Delta NRF2}$ and $Il4^{GFP}$ littermate controls. While the levels of ST2 were similar on day 3, we found a modest yet significant reduction in ST2 expression on IL-4-GFP^+ T cells in the lung of $Il4^{GFP}CD4^{\Delta NRF2}$ mice compared to their littermate controls on day 9 (Fig. 3*F*), suggesting a role for NRF2 in facilitating the optimal expression of ST2 on Th2 cells in the lung during allergic asthma. Levels of epithelial alarmin cytokines TSLP, IL-25, and IL-33 in the lung lysates were comparable between $CD4^{\Delta NRF2}$ and littermate control mice (Fig. 3*G*). Notably, when subjected to intranasal PAO/Ova challenge, $CD4^{\Delta NRF2}$ mice displayed more severe defects in the frequencies of IL-5^+, IL-13^+, IL-5^+IL-13^+ Th2 cells, as well as the levels of type 2 cytokines and the number of eosinophils in the BAL fluid, compared to $Il1rl1^{-/-}$ mice (Fig. 3 *H*–*J*). Based on these findings, we formulated the hypothesis that NRF2 induces the differentiation of polyfunctional Th2 cell in an IL-33/ST2-independent manner. To test this hypothesis, we differentiated naive $CD4^+$ T cells from WT or $Il1rl1^{-/-}$ mice into Th2 cells and restimulated them with IL-25 or IL-33 (Fig. 3*K*). As expected, IL-25 increased the frequency of IL-13^+ cells, while IL-33 failed to do so in the $Il1rl1^{-/-}$ Th2 cells. However, when we added ML385, we observed a significant decrease in the frequency of IL-13^+ producers in $Il1rl1^{-/-}$ Th2 cells under all restimulation conditions tested (Fig. 3 *L* and *M*). Collectively, these results strongly suggest that cell-intrinsic activation of NRF2 promotes the differentiation of polyfunctional Th2 cells in the lungs independently of the IL-33/ST2 pathway, while having little impact on the generation of initial Th2 cell commitment in the lymph node.

NRF2 Is Essential for Metabolic Fitness Required in Polyfunctional Th2 Cells. To gain mechanistic insights into the role of NRF2 in polyfunctional Th2 cells, we isolated $CD4^+$ T cells from the lungs of allergen-challenged $CD4^{\Delta NRF2}$ and littermate mice and subjected them to single-cell RNAseq analysis (*SI Appendix*, Fig. S5*A*). In total, 16,570 genes across 7,590 cells passed the quality control process and were used for differentially expressed genes (DEG) analysis and clustering. We used uniform manifold approximation projection (UMAP) to group cells with similar transcriptome profiles into clusters, which revealed ten transcriptionally distinct clusters such as

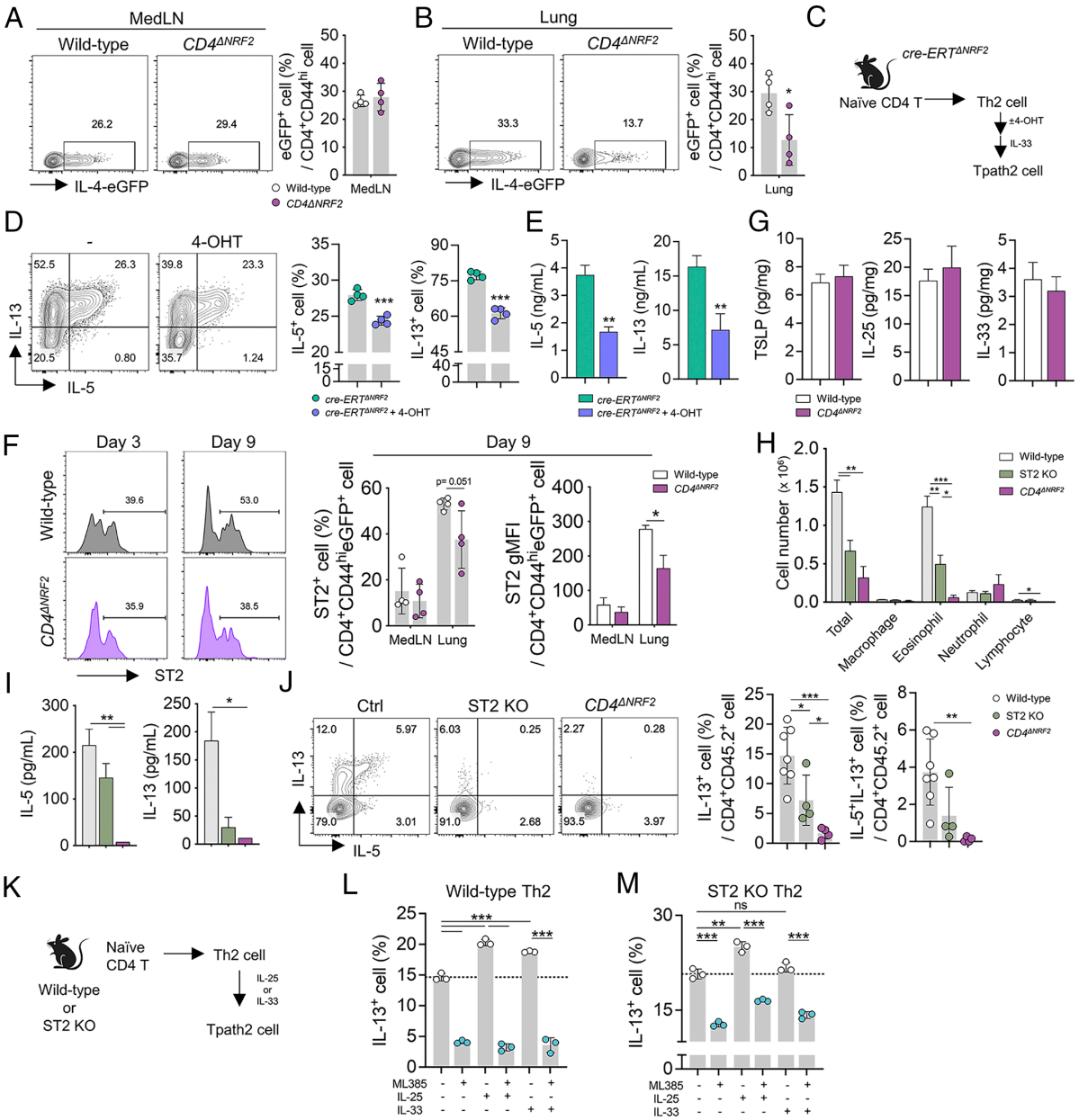

Fig. 3. NRF2 facilitates the differentiation of polyfunctional Th2 cell in an IL-33-independent manner. (*A* and *B*) *Il4*^{GFP}*CD4*$^{\Delta NRF2}$ and *Il4*^{GFP} mice were subjected to PAO/Ova-induced allergic asthma. Representative contour plots and quantifications of IL-4eGFP-expressing cells in the medLN (*A*) and the lung (*B*) of the indicated mice. (*C*–*E*) Schematic representation of Th2 cell restimulation study (*C*) and representative contour plots and quantification of IL-5- and/or IL-13-expressing cells upon restimulation (*D*). Quantification of IL-4, IL-5, and IL-13 in the culture supernatant (*E*). (*F* and *G*) *Il4*^{GFP}*CD4*$^{\Delta NRF2}$ and *Il4*^{GFP} mice were subjected to PAO/Ova-induced allergic asthma. The frequency or mean fluorescence intensity of ST2 in IL-4eGFP-expressing CD4$^+$ T cells (*F*), and quantification of TSLP, IL-25, and IL-33 in the lung tissue lysate (day 3) (*G*) from the indicated mice. The histogram shows representative plots in the lung. (*H*–*J*) Comparative analysis of WT ST2 knockout (KO), and *CD4*$^{\Delta NRF2}$ mice in a PAO/Ova-induced allergic asthma model. Differential cell counts (*H*), and the levels of IL-5 or IL-13 (*I*) in the BAL fluid. Representative plots and quantification of IL-13- and/or IL-5-expressing cells (*J*). (*K*–*M*) Schematic representation (*K*) and production of type 2 cytokines from WT (*L*) and ST2-deficient Th2 cells (*M*) stimulated under the indicated conditions. Data are representative of three independent experiments. Quantification plots show the means ± SD (*A*, *B*, *D*, *J*, *L*, and *M*) or ±SEM (*E*–*I*); ns: Not significant, *P < 0.05, **P < 0.01, and ***P < 0.001. Statistical analysis: unpaired Student's *t* test.

Th17 (cluster 0; *Rorc* and *Il17a*), Th2 (cluster 2; *Gata3, Il4, Il5,* and *Il13*), Treg (cluster 3; *Foxp3*), Th1 (cluster 5; *Tbx21* and *Ifng*), central memory-like (cluster 6; *Klf2* and *S1pr1*), and interferon-stimulated gene expressing (cluster 7; *Isg15,* and *Ifit1*) (Fig. 4*A* and *SI Appendix*, Fig. S5 *B*–*D*). Consistent with flow cytometric analyses and BAL fluid cytokine data, CD4$^+$ T cells from CD4$^{\Delta NRF2}$ mice consisted of less Th2 cells than littermates with a significant reduction in Th2-ness score calculated from *Il4*, *Il5*, *Il13*, *Gata3*, *Pparg*, *Il1rl1*, and *Areg* expression using Scanpy (Fig. 4 *B* and *C*) (31).

Hallmark pathway and subsequent gene set enrichment analyses (GSEA) with cells in cluster 2 (Th2) predicted that NRF2-deficient Th2 cells are relatively defective in multiple energy metabolism pathways including OXPHOS, glycolysis, fatty acid metabolism, and lipid oxidation (Fig. 4 *D* and *E*). In particular, the transcript levels of genes involved in OXPHOS and glycolysis were significantly lower in NRF2-deficient Th2 cells compared to NRF2-sufficient ones (*SI Appendix*, Fig. S6 *A* and *B*). Bulk RNA-seq analysis of in vitro-generated NRF2-deficient Th2 cells confirmed a broad defect in the expression of genes related to OXPHOS and glycolysis (Fig. 4*F*). To understand the mechanism underlying NRF2-mediated regulation of these genes, we performed assay of transposase-accessible chromatin with high-throughput sequencing (ATAC-seq) on WT and NRF2-deficient Th2 cells. Our analysis defined both decreased (n = 731) or increased (n = 294) peaks,

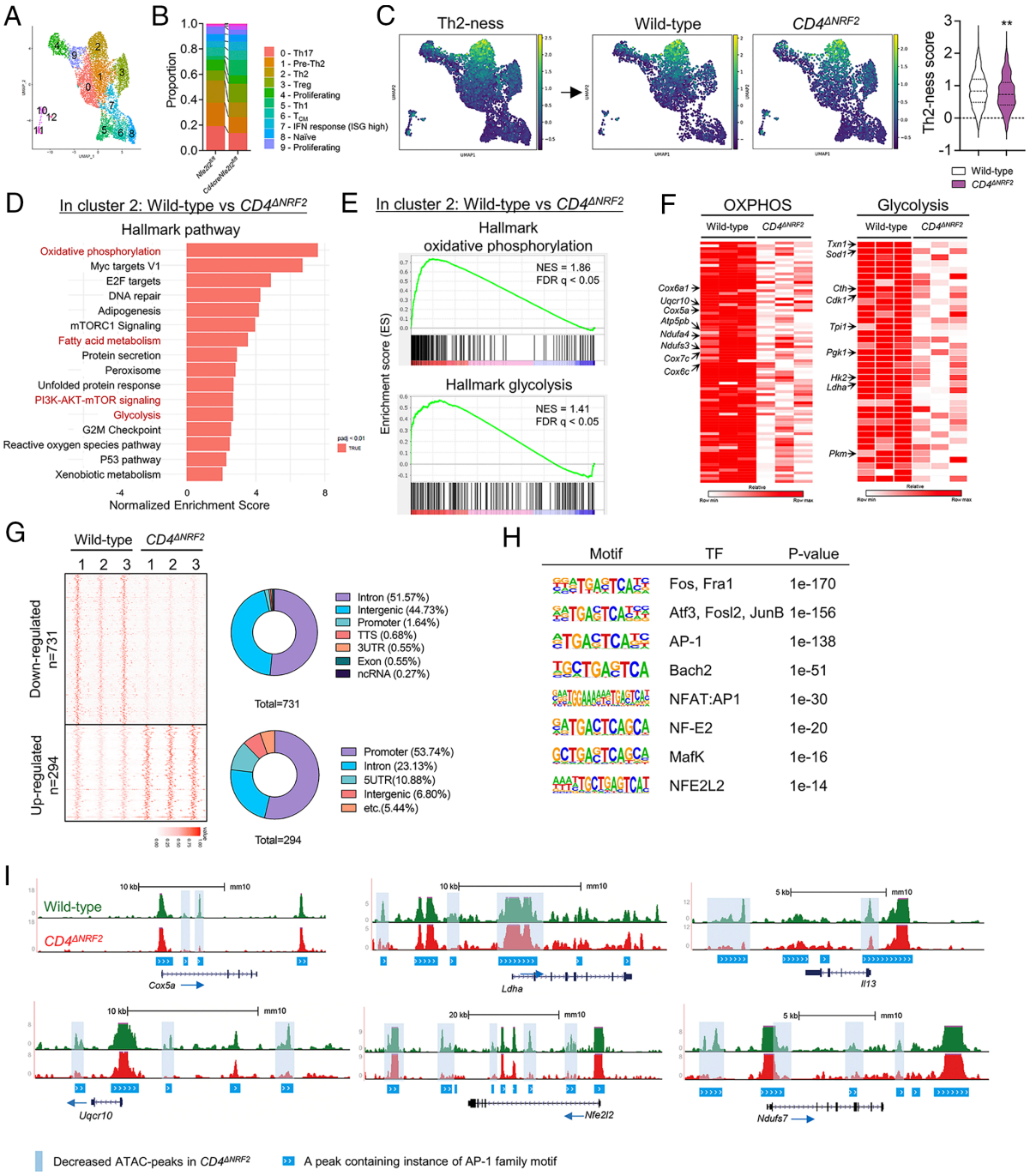

Fig. 4. NRF2 regulates the expression of genes associated with oxidative phosphorylation and glycolysis in Th2 cells. (*A–E*) *CD4*$^{\Delta NRF2}$ and WT mice were challenged with intranasal PAO/Ova, and CD4$^+$ T cells isolated from the lung were subjected to single-cell RNA-sequencing. UMAP plot (*A*), proportion graph (*B*), and Th2-ness UMAP and score (*C*). Hallmark pathway (*D*) and GSEA (*E*) of cluster 2. (*F–I*) Naive CD4$^+$ T cells from the indicated mice were differentiated under Th2-skewing condition and were subjected to bulk RNA-sequencing (*F*) or ATAC sequencing (*G–I*). (*F*) Heatmaps for oxidative phosphorylation- and glycolysis-related genes. Down-regulated or up-regulated peaks of ATAC-seq between the two groups (*G*), and motif enrichment analysis of downregulated ATAC-seq peaks in NRF2-deficient Th2 cells (*H*). Representative tracks based on ATAC-seq data obtained for the regions in proximity of the indicated genes (*I*). Peaks containing instance of AP-1 family motif are shown.

indicating dynamic chromatin remodeling associated with NRF2-deficiency in Th2 cells (Fig. 4*G*). Most down-regulated peaks were found in potential enhancers including intron and intergenic regions, while up-regulated peaks were primarily located at promoter regions. As expected, the NRF2-binding motif site was surrounded by reduced ATAC-seq signals in NRF2-deficient Th2 cells (*SI Appendix*, Fig. S6*C*). Of note, our de novo motif analysis of ATAC-seq revealed that NRF2 (NFE2L2) motifs were weakly enriched in down-regulated regions in NRF2-deficient Th2 cells, while activator protein-1 (AP-1) family motifs, such as Fos, Fra1, Atf3, Fosl2, and JunB, were strongly enriched (Fig. 4*H*). Furthermore, the down-regulated genes involved in OXPHOS and glycolysis were found to have multiple AP-1 family motifs (Fig. 4*I*). These results imply that NRF2 deficiency affects the binding of AP-1 transcription factors to the gene loci involved in OXPHOS and glycolysis, thereby altering the metabolic fitness of Th2 cells.

Consistent with their transcriptome features, NRF2-deficient Th2 cells had a significantly decreased OXPHOS activity as measured by O_2 consumption rate (OCR). In particular, the basal OCR in NRF2-deficient Th2 cells was remarkably diminished

(Fig. 5*A*). Additionally, NRF2-deficient Th2 cells displayed a moderate but significant decrease in glycolysis and glycolytic capacity (Fig. 5*B*), which correlated with a significant reduction of glucose uptake (Fig. 5*C*). BODIFY FL C_{16} staining analysis revealed that the uptake of fatty acids was not impaired in NRF2-deficient Th2 cells as well as in ML385-treated Th2 cells (Fig. 5*D*). Glucose and acetate serve as a substrate for cellular glycolysis and the tricarboxylic acid (TCA) cycle, respectively (32–35). The addition of acetate almost completely restored the frequency of IL-13$^+$ cells among NRF2-deficient Th2 cells, while high doses of glucose partially but significantly increased it (Fig. 5 *E* and *F*). Similarly, the inclusion of acetate and glucose remarkably increased the frequency of IL-13$^+$ cells in Th2 cells differentiated in the presence of ML385 (Fig. 5*G*). In WT CD4$^+$ T cells, addition of acetate, but not high-dose glucose, increased the frequency of IL-13$^+$ cells (*SI Appendix*, Fig. S6*D*). Collectively, these results strongly suggest that T cell–intrinsic NRF2 induces optimal OXPHOS and glycolytic activity to drive the differentiation of polyfunctional Th2 cells.

PPARγ Is Involved in NRF2-Mediated Polyfunctionality of Th2 Cells. Analysis of Th2-related transcription factors in cluster 2 revealed that NRF2-deficient Th2 cells expressed normal levels of *Gata3, Irf4,* and *Xbp1* and an increased level of *Bhlhe40* but exhibited a significantly reduced level of *Pparg* (*SI Appendix*, Fig. S7*A*). In allergen-challenged *Il4*^{GFP} mice, IL-4-GFP$^+$ CD4$^+$ T cells in the lung expressed higher levels of *Gata3* and *Pparg* than those in the medLN (Fig. 6*A*). Interestingly, while *Nfe2l2* expression levels were comparable between PPARγ-deficient and PPARγ-sufficient Th2 cells, NRF2-deficient Th2 cells expressed a lower level of *Pparg* than NRF2-sufficient counterparts (Fig. 6*B*). During Th2 differentiation, NRF2-deficient CD4$^+$ T cells exhibited intact expression of *Pparg* at the early stage (by day 3) but failed to further increase its expression by day 4, leading to normal IL-4, but significantly reduced levels of IL-5 and IL-13 (Fig. 6 *C* and *D* and *SI Appendix*, Fig. S7*B*). Expression of *Gata3* was comparable between NRF2-sufficient and -deficient Th2 cells differentiated in vitro (Fig. 6*C*). These results collectively suggest that NRF2 is required for optimal PPARγ expression during Th2 cell differentiation. Intriguingly, treatment with troglitazone, a PPARγ agonist, dose-dependently increased the production of IL-5 and IL-13 in NRF2-deficient Th2 cells, comparable to the levels observed in NRF2-sufficient Th2 cells (Fig. 6*E*). Troglitazone boosted IL-5 and IL-13 production more profoundly in NRF2-deficient Th2 cells than in NRF2-sufficient ones (*SI Appendix*, Fig. S7 *C* and *D*). Furthermore, we observed that troglitazone treatment significantly elevated the basal respiration capacity and ATP production in NRF2-deficient Th2 cells, although the levels remained lower than those observed in NRF2-sufficient Th2 cells (Fig. 6*F*).

We further investigated whether treatment with a PPARγ agonist could also restore polyfunctional Th2 cell responses and subsequent allergic inflammation in CD4$^{\Delta NRF2}$ mice in vivo (Fig. 6*G*). We observed that administration of troglitazone resulted in a remarkable increase in the numbers of eosinophils in the BAL fluid (Fig. 6 *H* and *I*) as well as the infiltration of inflammatory cells and mucus-producing goblet cells in the lung of CD4$^{\Delta NRF2}$ mice (Fig. 6*J*). Importantly, troglitazone treatment partially but significantly restored the frequencies of IL-5- and IL-13-producing polyfunctional Th2 cells in these mice (Fig. 6*K*). These findings suggest that PPARγ is involved in NRF2-mediated differentiation of polyfunctional Th2 cells, potentially by contributing to OXPHOS activity. Nevertheless, the observation that NRF2-deficient Th2 cells exhibited a more pronounced reduction in IL-13 compared to PPARγ-deficient Th2 cells in vitro, and that troglitazone only partially restored

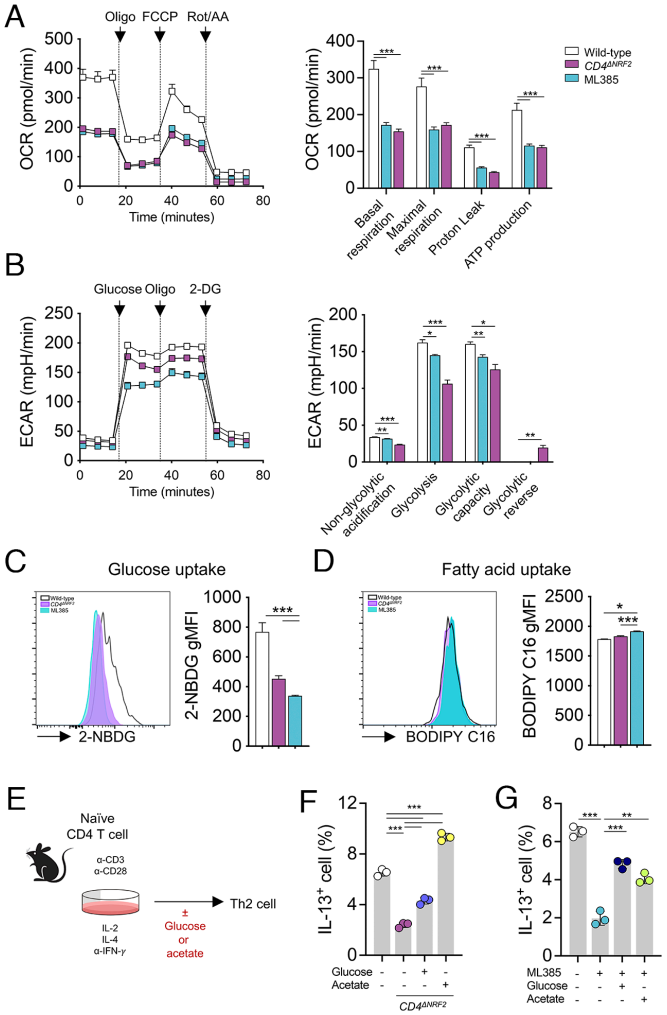

Fig. 5. NRF2-driven metabolic fitness is essential for polyfunctional Th2 cell differentiation. (*A–D*) Naive CD4$^+$ T cells from *CD4*$^{\Delta NRF}$ and WT mice were differentiated under Th2-skewing condition in the presence or absence of ML385. The cells were subjected to extracellular flux analysis, and OCR (*A*) and ECAR (*B*) results were shown. Histogram and gMFI of 2-NBDG (*C*) or BODIPY C16 (*D*) uptake by the cells were analyzed. (*E–G*) Naive CD4$^+$ T cells from *CD4*$^{\Delta NRF2}$ and WT mice were differentiated under Th2-skewing condition in the presence or absence of glucose or acetate. Experimental scheme (*E*), and the frequency of IL-13-producing cells are shown (*F* and *G*). Data are representative of three independent experiments. Quantification plots show the means + SEM (*A–D*) or ±SD (*F* and *G*); **P* < 0.05, ***P* < 0.01, and ****P* < 0.001. Statistical analysis: unpaired Student's *t* test.

Th2 immunity in CD4$^{\Delta NRF2}$ mice in vivo, suggests the possibility of a PPARγ-independent role of NRF2 in Th2 cells.

NRF2 Is Crucial for IL-5 and IL-13 Production from Human Th2 Cells. To elucidate the role of NRF2 in human Th2 cells, we stimulated human naive CD4$^+$ T cells under Th2-skewing condition with or without the NRF2 inhibitor ML385 (Fig. 7*A*). Consistent with our findings in murine CD4$^+$ T cells, ML385 treatment significantly reduced the frequencies of IL-5 and/or IL-13-producing cells, as well as the levels of these cytokines in culture supernatant (Fig. 7 *B* and *C*). Moreover, extracellular flux analysis showed that ML385 treatment led to a significant decrease in the basal and maximal respiration capacity of human Th2 cells (Fig. 7*D*). Notably, ML385 treatment also resulted in a remarkable decrease in the glycolysis and glycolytic capacity, which was more pronounced compared to the moderate reduction observed in murine Th2 cells (Fig. 7*E*). Furthermore, the expression of glycolysis-related genes, such as *ALDOA*, *PGK1*, *ENO1*, and *PKM2*, was significantly inhibited

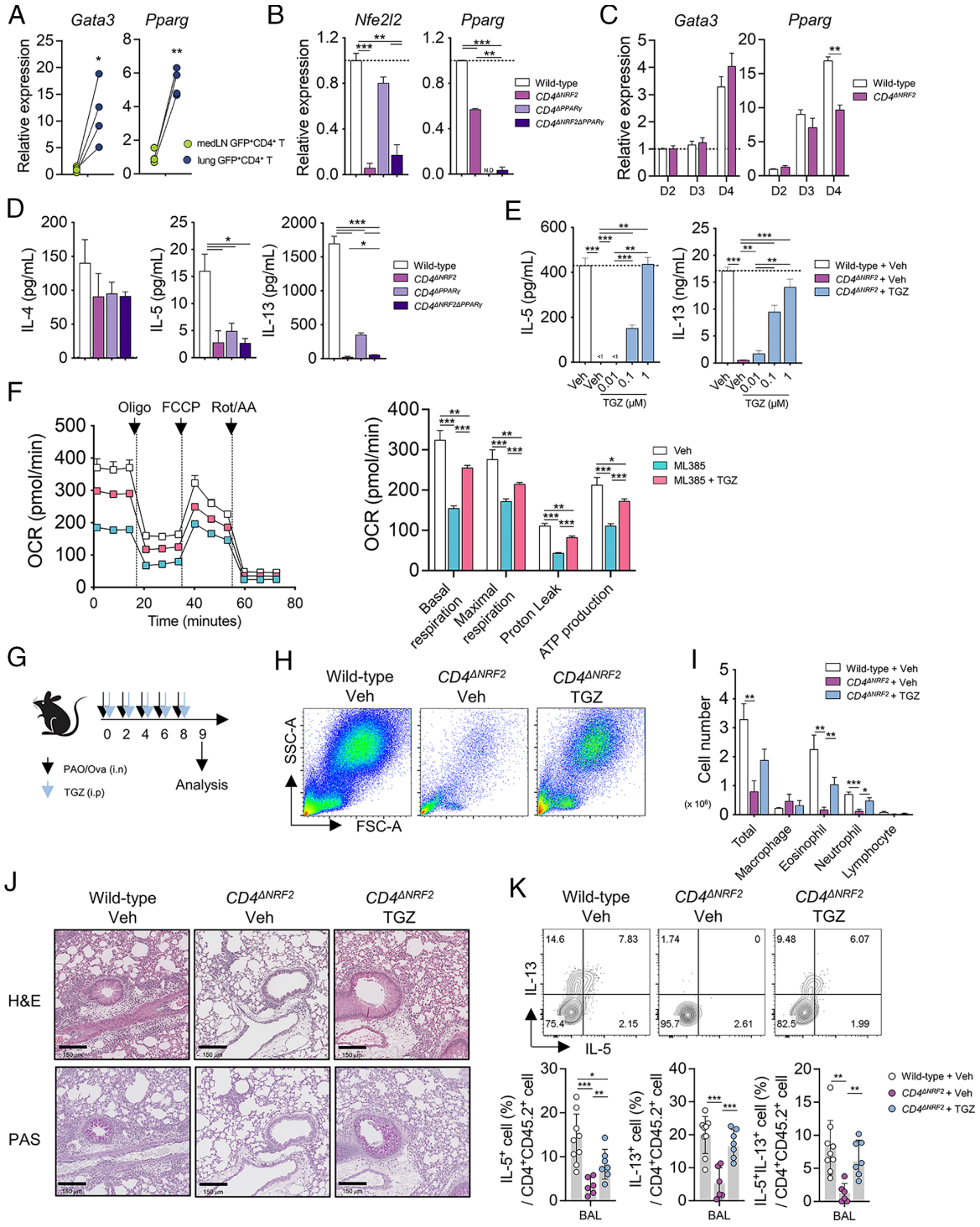

Fig. 6. PPARγ reinstates polyfunctionality of Th2 cells in the absence of NRF2. (*A*) *Il4*^{GFP} mice were intranasally challenged with PAO/Ova, and the levels of *Gata3* and *Pparg* transcript in IL-4eGFP-expressing CD4$^+$ T cells in the medLN or the lungs were analyzed. (*B–D*) Naive CD4$^+$ T cells from the indicated mice were cultured under a Th2-skewing condition for 4 d. Relative expression of *Nfe2l2* or *Pparg* (*B*), the kinetics of *Gata3* and *Pparg* expression (*C*), and the levels of IL-4, IL-5, and IL-13 in the supernatant (*D*). (*E*) Naive CD4$^+$ T cells from WT or *CD4*$^{\Delta NRF2}$ were cultured under a Th2-skewing condition with or without troglitazone (TGZ), and the levels of IL-5 and IL-13 in the supernatant were analyzed. (*F*) Seahorse analysis to assess OCR in Th2 cells after differentiation with indicated conditions. (*G–K*) *CD4*$^{\Delta NRF2}$ and WT were subjected to PAO/Ova-induced allergic asthma, and additionally given troglitazone or vehicle (i.p.). Schematic representation (*G*), and representative FSC/SSC FACS plots (*H*) or differential cell counts (*I*) of the BAL fluid cells. H&E and PAS staining of the lung (*J*) or representative contour plots and quantification of IL-5- and/or IL-13-expressing cells in CD45.2$^+$CD4$^+$ T cells in BAL fluid (*K*). Data are representative of three independent experiments. Quantification plots show the means ± SEM (*B–F*, and *I*) or ±SD (*K*); *P < 0.05, **P < 0.01, and ***P < 0.001. Statistical analysis: paired Student's *t* test (*A*), unpaired Student's *t* test (*B–F*, *I*, and *K*).

in ML385-treated human Th2 cells (*SI Appendix*, Fig. S8*A*). The addition of either acetate or high doses glucose almost completely restored IL-5 and IL-13 production in ML385-treated human Th2 cells, indicating that the NRF2 inhibitor diminished cytokine production by impairing OXPHOS and glycolytic capacity (Fig. 7*F*). Quantitative PCR analysis demonstrated that ML385 treatment significantly reduced the expression of *IL5*, *IL13*, and to a lesser extent, *PPARG* in human Th2 cells (*SI Appendix*, Fig. S8*B*). The addition of troglitazone effectively restored the production of IL-5 and IL-13, as well as the expression of *GATA3*, *IL5*, and *IL13*

transcript, in ML385-treated human Th2 cells, corroborating our findings in murine Th2 cells (Fig. 7*G*).

Finally, we investigated whether NRF2 played a role in the production of IL-5 and IL-13 in allergen-specific Th2 cells derived from asthmatic patients. Peripheral blood mononuclear cells (PBMCs) isolated from *Dermatophagoides farina*-reactive asthma patients were stimulated with *D. farinae* extract in the presence of ML385 or vehicle (Fig. 7*H*). As anticipated, cells from asthma patients secreted IL-5 and IL-13 in response to the stimulation, unlike those from healthy individuals (*SI Appendix*, Fig. S8*C*). As depicted in Fig. 7*I*, ML385 significantly reduced the production of IL-5 and IL-13 in these allergen-specific human effector/memory Th2 cells. Overall, these findings highlight the crucial role of NRF2 in promoting the differentiation and function of human Th2 cells, while emphasizing the close association between NRF2 activity and the metabolic state of these cells.

Discussion

Using multiple murine and human allergic asthma models, we propose that NRF2 is a T cell–intrinsic factor that is essential for driving polyfunctionality of Th2 cells in the lung based on our findings that i) blockade of either ROS or NRF2 significantly inhibited both eosinophilia and polyfunctional Th2 cells in the lung, ii) mice lacking NRF2 exclusively in T cells failed to develop polyfunctional Th2 cells in the lung but had normal IL-4-producing T cells in the lymph nodes, iii) T cell expression of NRF2 was required for optimal OXPHOS and glycolysis capacity as well as PPARγ expression to drive IL-5 and IL-13 expression, iv) blockade of NRF2 reduced IL-5 and IL-13 production from HDM allergen-specific human Th2 cells obtained from asthma patients. Thus, the present study demonstrates that NRF2 acts as an essential spatiotemporal metabolic hub required for inducing the differentiation of polyfunctional Th2 cells.

Upon TCR signaling, T cells are known to increase intracellular ROS from mitochondria within a few minutes (36). While ROS has been suggested to promote T cell signaling through ERK (19, 37), the exact role of intracellular ROS in T cells in in vivo settings remains incompletely understood as most studies have exposed T cells to exogenous oxidative stress in in vitro TCR-cross-linking systems. The present study found that the level of intracellular ROS in T cells was similarly elevated in the allergen-challenged lung in both $CD44^{hi}$ and $CD44^{lo}$ subsets when compared with that of the medLNs. Our findings demonstrate that ROS–NRF2 axis crucially contributes to type 2 inflammation in vivo, as demonstrated by the profound amelioration of eosinophilia and mucus production in the airway by NAC and ML385. While NAC is known for its antioxidant properties, studies suggest it can also boost NRF2 expression(38, 39). It's unclear whether NAC improves eosinophilic asthma by regulating NRF2 expression in this study. Studies with various cell-type-specific NRF2-deficient mice as well as mixed bone-marrow chimeras revealed the essential T cell-intrinsic role of NRF2 in polyfunctional Th2 cells. This role of NRF2 in driving polyfunctional Th2 cells is surprising since NRF2-germline knockout mice have been reported to be more susceptible to allergic asthma (40, 41).

How NRF2 drives polyfunctionality in Th2 cells? Through scRNA transcriptome analysis, we found that in vivo generated NRF2-deficient Th2 cells have impaired expression of genes associated cellular energy metabolism pathways, such as OXPHOS and glycolysis. Supplementation with acetate or high-dose glucose significantly restored the expression of IL-5 and IL-13 in NRF2-deficient Th2 cells, indicating that defective OXPHOS and glycolysis resulted in defective polyfunctionality in the NRF2-deficient Th2 cells, as well as in Th2 cells cultured in the presence of an NRF2 inhibitor. Among helper T cell subsets, Th2 cells are the most glycolytic subsets with the highest expression of Glut1 and perturbation of glycolysis reduces IL-13 production by Th2 cells (42). PPARγ appeared to have a role in NRF2-mediated OXPHOS in Th2 cells. NRF2 has been shown to directly induce *Pparg* by binding on its -784 antioxidant response elements (ARE) in lung epithelial cells (43). The motif analysis of ATAC peaks identified that a significant enrichment of the binding motifs of various AP-1 family transcription factors in WT Th2 cells was diminished in NRF2-deficient counterparts. AP-1 has been shown to regulate the expression of the gene encoding hexokinase, which catalyzes the first step of the glycolytic pathway and glucose uptake in a T cell line (44). It is worth noting that the NRF2 binding site (ARE) and the AP-1 binding site (TRE) often intersect, giving rise to a composite NRF2/AP-1 site (45, 46). Thus, the present study proposes that NRF2 induces the optimal OXPHOS and glycolytic activity in Th2 cells by inducing genes involved in the bioenergetic metabolic pathways through AP-1 family transcription factors.

Epithelial cytokines TSLP, IL-25, and IL-33 play a crucial role in the differentiation and expansion of type 2 immune cells. IL-33, in particular, has been shown to exacerbate allergic lung inflammation by promoting the expansion of ILC2s and inducing the expression of IL-5 and IL-13 in Th2 cells (1, 47, 48). Given that ST2 expression is selectively increased on memory Th2 cells, IL-33 induces the production of IL-5 from memory Th2 cells, but not from effector Th2 cells (14). $CD4^{\Delta NRF2}$ mice showed more significant reduction in eosinophilia and polyfunctional Th2 cells in the airway compared to *Il1rl1*$^{-/-}$ mice. NRF2 blockade had little effect on the frequency of $IL\text{-}5^{+}IL\text{-}13^{+}$ ILC2s challenged with intranasal papain, which is known to depend on IL-33 (49). Moreover, blockade of NRF2 efficiently inhibited the expression of IL-5 and IL-13 in *Il1rl1*$^{-/-}$ $CD4^{+}$ T cells. Therefore, we propose that NRF2 and IL-33 differentially promote allergic inflammation in vivo; NRF2 is activated when initial Th2 cells migrate into the inflamed lung and drive the polyfunctionality by facilitating OXPHOS and glycolysis, while IL-33 acts on memory Th2 cells and ILC2 to induce the production of type 2 cytokines. The level of ST2 on lung Th2 cells was diminished in $CD4^{\Delta NRF2}$ mice compared to WT littermates at day 9. Thus, optimal expression of ST2 on lung Th2 cells is partially dependent on NRF2. This NRF2-mediated upregulation of ST2 is possibly through the induction of PPARγ (50, 51).

The identification of a direct connection between cellular redox status and Th2 provides a unique T cell–intrinsic mechanism that underlies spatiotemporal epigenetic and metabolic reprogramming, resulting in the induction of polyfunctionality of the cells. It will be intriguing to explore whether similar mechanisms are applicable to other allergic diseases or other subsets of helper T cells. Targeting NRF2 and redox pathway by using small molecules is an active area of research for developing anticancer therapeutics (52, 53). Our findings suggest that targeting ROS–NRF2–OXPHOS/glycolysis pathway may be effective in the treatment of allergic diseases by inhibiting polyfunctional potential of Th2 cells.

Materials and Methods

A full description of the materials and methods is available in *SI Appendix*.

Animals. C57BL/6 (CD45.2; CrlOri) mice were purchased from the Orient Bio. *Nfe2l2*$^{fl/fl}$ (C57BL/6-*Nfe2l2*$^{tm1.1Sred}$/SbisJ; 025433), 4get, *Itgax-cre* (B6.Cg-Tg(Itgax-cre)1-1Reiz/J; 008068), B6.SJL(B6.SJL-*Ptprc*^{a} *Pepc*^{b}/BoyJ; 002014), and *Rag1*$^{-/-}$ (B6.129S7-*Rag1*^{tm1Mom}/J; 002216) mice were purchased from Jackson Laboratory. *Cd4cre*, *Pparg*$^{fl/fl}$, and *Foxp3*$^{YFP\text{-}Cre}$ mice were kindly provided by Dr. Chen Dong (Tsinghua University, China), Dr. Je-Min Choi (Hanyang University, Korea), and Dr. Jae-Hoon Chang (Yeungnam University, Korea), respectively. ST2 knockout mice were kindly provided by Drs. Andrew N. Mckenzie (MRC

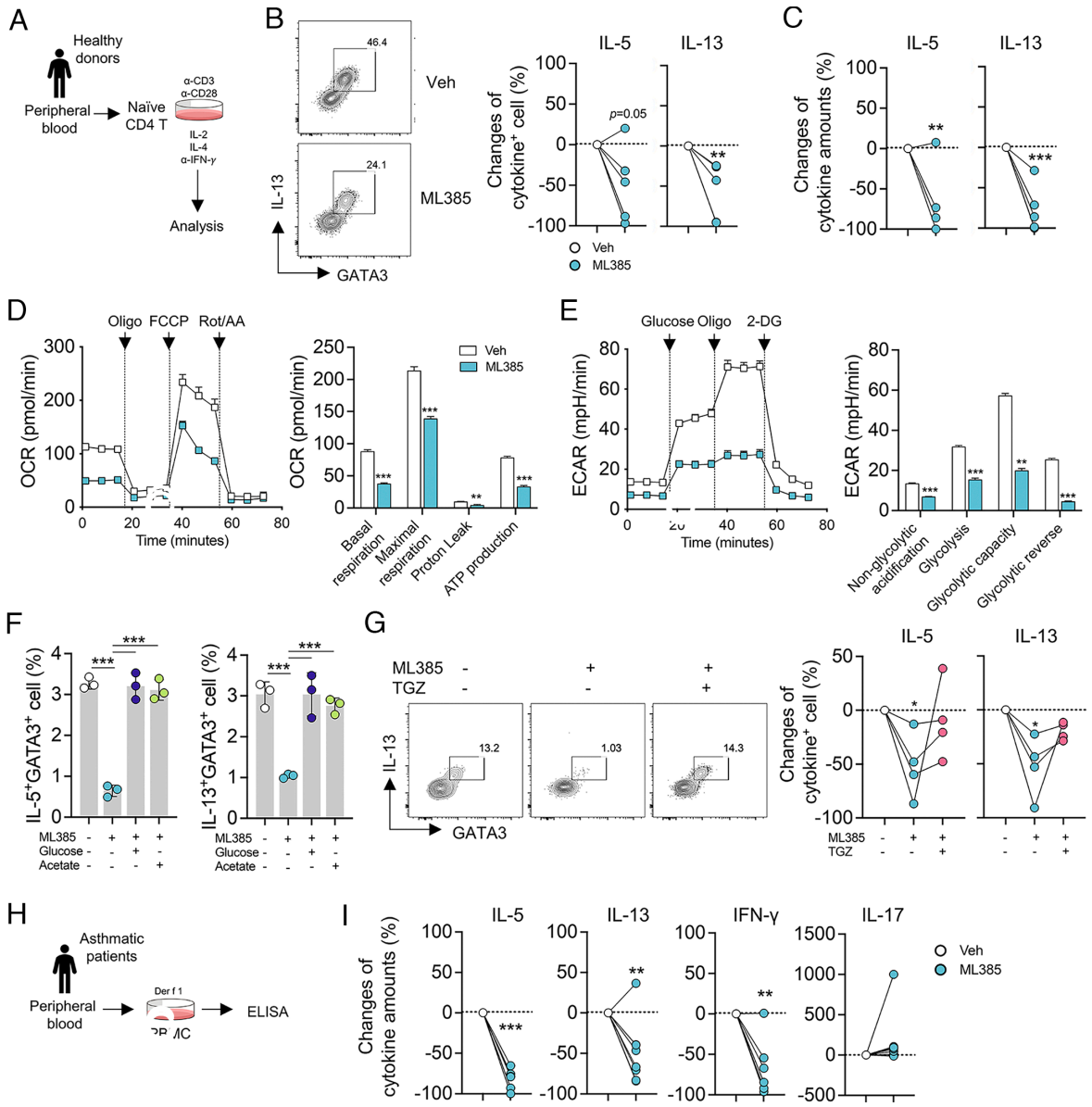

Fig. 7. NRF2 inhibition hampers OXPHOS, glycolysis, and IL-5/IL-13 production in human Th2 cells. (*A*–*E*) Naive CD4$^+$ T cells from healthy donors were cultured under a Th2-skewing condition with ML385 or vehicle. Schematic representation (*A*) and representative contour plots of IL-5- or IL-13-expressing cells and changes of cytokine-producing cells (*B*) or the levels of indicated cytokines in the supernatant (*C*) after ML385 treatment, and the OCR (*D*) and ECAR (*E*) analysis are shown. (*F* and *G*) Naive CD4$^+$ T cells from healthy donors were cultured under a Th2-skewing condition in the presence or absence of ML385, glucose, acetate, and/or troglitazone, as indicated. The frequencies of IL-5 or IL-13 cells (*F*) or the changes of cytokine-producing cells (*G*) were analyzed. (*H* and *I*) PBMCs from Der f1-reactive asthmatic patients were stimulated with Der f1 in the presence or absence of ML385. Schematic representation (*H*), and the changes of indicated cytokines upon ML385 treatment (*I*). Data are representative of three independent experiments. Quantification plots show the means ± SEM (*D* and *E*) or ±SD (*F*); *P < 0.05, **P < 0.01, and ***P < 0.001. Statistical analysis: paired Student's t test (*B*, *C*, *G*, and *I*), unpaired Student's t test (*D*–*F*).

Laboratory of Molecular Biology) and Sang-Jun Ha (Yonsei University, Korea). *Cd4cre*, *Itgax-cre*, *Foxp3*$^{YFP\text{-}Cre}$, and 4get mice were crossed to *Nfe2l2*$^{fl/fl}$ mice to construct NRF2 conditional knockout mice. All animal experiments were approved by the Institutional Animal Care and Use Committee of Seoul National University and conducted in accordance with the guidelines of Seoul National University for the care and use of laboratory animals (IACUC No.: SNU-220930-3). For animal experiments, age- and sex-matched 8- to 15-wk-old mice were used and all mice were maintained in the Animal Center for Pharmaceutical Research of Seoul National University under specific pathogen-free conditions.

Human Subjects. Collection of human blood samples from healthy volunteers and subsequent experimental procedures were reviewed and approved by the Seoul National University Institutional Review Board (IRB No.: 2205/001-006). Allergic asthmatic patients (n = 6) enrolled in this study were provided with written informed consent, and the study protocol was approved by the Seoul National University Hospital Institutional Review Board (IRB No.: 1810-036-977).

Allergen-Induced Lung Inflammation Models. Mice were anesthetized with isoflurane and intranasally administrated with a mixture of 7 ug of PAO and 20 μg of Ova every other day for 9 d (days 0, 2, 4, 6, and 8). In HDM-induced lung inflammation experiments, mice were sensitized on day 0 by 1 μg of Der f 1 via intranasal route. After 1 wk, mice were intranasally administered with 10 μg of Der f 1 every day for a total five times (days 7, 8, 9, 10, and 11). Sixteen hours after the last administration, all mice were killed and BAL fluid, lung, and mediastinal lymph node were obtained for further analysis.

For mixed bone marrow transplantation experiment, donor bone marrow cells from WT control (CD45.1$^{+/+}$) and CD4$^{\Delta NRF2}$ (CD45.2$^{+/+}$) mice were mixed at 1:1 ratio and adoptively transferred into irradiated recipient *Rag1*$^{-/-}$ mice. After a 4-wk reconstitution period, the recipients were intranasally injected with a mixture of PAO/Ova.

For histologic analysis, mice were exsanguinated and their lungs were incubated in 10 % formalin solution (Sigma) for overnight at 4 °C for fixation then embedded in paraffin. 5 μm thick sections were cut from paraffin embedded lung

with a microtome and stained with PAS or H&E staining kit, and the samples were visualized by Aperio AT2 (Leica, Wetzlar, Germany). To collect BAL fluid from the mouse, the airway lumen was rinsed twice using 0.8 mL of PBS after cannulating the trachea. The obtained BAL fluid underwent centrifugation to separate supernatant from cells in the pellet, which were then resuspended in dPBS. Subsequently, approximately 10,000 cells were attached to slide glass via cytospin and stained with DiffQuik (Baxter Healthcare, Compton, UK) following the manufacturer's instruction.

Data, Materials, and Software Availability. scRNA-seq, bulk RNA-seq, and ATAC-seq data have been deposited in NCBI GEO repository (GSE241355 and GSE241138) (54, 55).

ACKNOWLEDGMENTS. We thank Dr. Chen Dong (Tsinghua University) for *Cd4cre*mice, Dr. Je-Min Choi (Hanyang University) for *Pparg*$^{fl/fl}$mice, Drs. Andrew N. Mckenzie (Medical Research Council (MRC) Laboratory of Molecular Biology) and Sang-Jun Ha (Yonsei University) for ST2 knockout mice, and Dr. Jae-Hoon Chang (Yeungnam University) for *Foxp3*$^{YFP\text{-}Cre}$mice. We also thank the entire Chung lab members and Dr. Je-Min Choi for their discussion and suggestion. This work was supported by Grants NRF-2020R1A3B2078890 (Y.C.), NRF-2022R1A6A1A03046247 (Y.C.), and NRF-201R1A6A3A01086970 (G.C.) from National Research Foundation of Korea.

Author affiliations: [a]Laboratory of Immune Regulation, Institute of Pharmaceutical Sciences, College of Pharmacy, Seoul National University, Seoul 08826, Republic of Korea; [b]Division of Life Sciences, College of Life Sciences and Bioengineering, Incheon National University, Incheon 22012, Republic of Korea; [c]Laboratory of Mucosal Immunology in Department of Biomedical Sciences, Seoul National University College of Medicine, Seoul 03080, Republic of Korea; [d]Laboratory of Molecular Immunology, Department of Biological Science, Ulsan National Institute of Science & Technology, Ulsan 44919, Republic of Korea; [e]College of Pharmacy and Integrated Research, Institute for Drug Development, Dongguk University, Goyang 10326, Republic of Korea; and [f]Graduate School of Medical Science and Engineering, Korea Advanced Institute of Science and Technology, Daejeon 34141, Republic of Korea

Author contributions: G.C., J.B., H.Y.K., and Y.C. designed research; G.C., J.B., J.C., J.W.S., H.O., Y.J., J.K., D.K., H.M., J.-E.L., and S.H.P. performed research; H.-Y.J., H.O., Y.-S.K., Y.-M.K., H.Y.K., S.H.P., and M.-R.H. contributed new reagents/analytic tools; G.C., H.-Y.J., J.B., J.C., H.O., M.-R.H., and Y.C. analyzed data; and G.C., H.-Y.J., Y.-M.K., M.-R.H., and Y.C. wrote the paper.

1. P. Licona-Limon, L. K. Kim, N. W. Palm, R. A. Flavell, TH2, allergy and group 2 innate lymphoid cells. *Nat. Immunol.* **14**, 536–542 (2013).
2. T. Nakayama *et al.*, Th2 cells in health and disease. *Annu. Rev. Immunol.* **35**, 53–84 (2017).
3. K. Nistala *et al.*, Th17 plasticity in human autoimmune arthritis is driven by the inflammatory environment. *Proc. Natl. Acad. Sci. U.S.A.* **107**, 14751–14756 (2010).
4. A. Penatti *et al.*, Differences in serum and synovial CD4+ T cells and cytokine profiles to stratify patients with inflammatory osteoarthritis and rheumatoid arthritis. *Arthritis Res. Ther.* **19**, 103 (2017).
5. J. A. Walker, A. N. J. McKenzie, T(H)2 cell development and function. *Nat. Rev. Immunol.* **18**, 121–133 (2018).
6. S. L. Swain, K. K. McKinstry, T. M. Strutt, Expanding roles for CD4(+) T cells in immunity to viruses. *Nat. Rev. Immunol.* **12**, 136–148 (2012).
7. S. T. Smale, A. G. Fisher, Chromatin structure and gene regulation in the immune system. *Annu. Rev. Immunol.* **20**, 427–462 (2002).
8. V. A. Rathinam, S. K. Vanaja, K. A. Fitzgerald, Regulation of inflammasome signaling. *Nat. Immunol.* **13**, 333–342 (2012).
9. S. J. Van Dyken *et al.*, A tissue checkpoint regulates type 2 immunity. *Nat. Immunol.* **17**, 1381–1387 (2016).
10. N. L. Bertschi, C. Bazzini, C. Schlapbach, The concept of pathogenic TH2 cells: Collegium internationale allergologicum update 2021. *Int. Arch. Allergy Immunol.* **182**, 365–380 (2021).
11. F. Buettner *et al.*, Computational analysis of cell-to-cell heterogeneity in single-cell RNA-sequencing data reveals hidden subpopulations of cells. *Nat. Biotechnol.* **33**, 155–160 (2015).
12. N. E. Mangan, A. Dasvarma, A. N. McKenzie, P. G. Fallon, T1/ST2 expression on Th2 cells negatively regulates allergic pulmonary inflammation. *Eur. J. Immunol.* **37**, 1302–1312 (2007).
13. M. Verma *et al.*, Experimental asthma persists in IL-33 receptor knockout mice because of the emergence of thymic stromal lymphopoietin-driven IL-9(+) and IL-13(+) type 2 innate lymphoid cell subpopulations. *J. Allergy Clin. Immunol.* **142**, 793–803.e798 (2018).
14. Y. Endo *et al.*, The interleukin-33-p38 kinase axis confers memory T helper 2 cell pathogenicity in the airway. *Immunity* **42**, 294–308 (2015).
15. K. H. Shalaby *et al.*, Inhaled birch pollen extract induces airway hyperresponsiveness via oxidative stress but independently of pollen-intrinsic NADPH oxidase activity, or the TLR4-TRIF pathway. *J. Immunol.* **191**, 922–933 (2013).
16. M. Cho *et al.*, Fibrinogen cleavage products and Toll-like receptor 4 promote the generation of programmed cell death 1 ligand 2-positive dendritic cells in allergic asthma. *J. Allergy Clin. Immunol.* **142**, 530–541.e536 (2018).
17. H. Na *et al.*, Concomitant suppression of T(H)2 and T(H)17 cell responses in allergic asthma by targeting retinoic acid receptor-related orphan receptor gammat. *J. Allergy Clin. Immunol.* **141**, 2061–2073.e2065 (2018).
18. J. M. Stark, C. A. Tibbitt, J. M. Coquet, The Metabolic Requirements of Th2 Cell Differentiation. *Front. Immunol.* **10**, 2318 (2019).
19. S. Devadas, L. Zaritskaya, S. G. Rhee, L. Oberley, M. S. Williams, Discrete generation of superoxide and hydrogen peroxide by T cell receptor stimulation: Selective regulation of mitogen-activated protein kinase activation and FAS ligand expression. *J. Exp. Med.* **195**, 59–70 (2002).
20. K. Gulow *et al.*, HIV-1 trans-activator of transcription substitutes for oxidative signaling in activation-induced T cell death. *J. Immunol.* **174**, 5249–5260 (2005).
21. S. Bergamini *et al.*, N-acetylcysteine inhibits in vivo nitric oxide production by inducible nitric oxide synthase. *Nitric Oxide* **5**, 349–360 (2001).
22. A. M. Sadowska, Y. K. B. Manuel, W. A. De Backer, Antioxidant and anti-inflammatory efficacy of NAC in the treatment of COPD: discordant in vitro and in vivo dose-effects: A review. *Pulm. Pharmacol. Ther.* **20**, 9–22 (2007).
23. M. Halasi *et al.*, ROS inhibitor N-acetyl-L-cysteine antagonizes the activity of proteasome inhibitors. *Biochem. J.* **454**, 201–208 (2013).
24. G. Aldini *et al.*, N-Acetylcysteine as an antioxidant and disulphide breaking agent: The reasons why. *Free Radic. Res.* **52**, 751–762 (2018).
25. E. Kansanen, S. M. Kuosmanen, H. Leinonen, A. L. Levonen, The Keap1-Nrf2 pathway: Mechanisms of activation and dysregulation in cancer. *Redox Biol.* **1**, 45–49 (2013).
26. I. Martinez-Gonzalez, C. A. Steer, F. Takei, Lung ILC2s link innate and adaptive responses in allergic inflammation. *Trends Immunol.* **36**, 189–195 (2015).
27. M. Kubo, Innate and adaptive type 2 immunity in lung allergic inflammation. *Immunol. Rev.* **278**, 162–172 (2017).
28. I. L. King, M. Mohrs, IL-4–producing CD4+ T cells in reactive lymph nodes during helminth infection are T follicular helper cells. *J. Exp. Med.* **206**, 1001–1007 (2009).
29. M. Kurowska-Stolarska *et al.*, IL-33 induces antigen-specific IL-5+ T cells and promotes allergic-induced airway inflammation independent of IL-4. *J. Immunol.* **181**, 4780–4790 (2008).
30. K. Oboki *et al.*, IL-33 is a crucial amplifier of innate rather than acquired immunity. *Proc. Natl. Acad. Sci. U.S.A.* **107**, 18581–18586 (2010).
31. F. A. Wolf, P. Angerer, F. J. Theis, SCANPY: Large-scale single-cell gene expression data analysis. *Genome Biol.* **19**, 15 (2018).
32. M. L. Balmer *et al.*, Memory CD8(+) T cells require increased concentrations of acetate induced by stress for optimal function. *Immunity* **44**, 1312–1324 (2016).
33. W. Li *et al.*, Hyperglycemia alters astrocyte metabolism and inhibits astrocyte proliferation. *Aging Dis.* **9**, 674–684 (2018).
34. C. I. Daien *et al.*, Gut-derived acetate promotes B10 cells with antiinflammatory effects. *JCI Insight* **6**, e144156 (2021).
35. Y. Hou *et al.*, CD36 promotes NLRP3 inflammasome activation via the mtROS pathway in renal tubular epithelial cells of diabetic kidneys. *Cell Death Dis.* **12**, 523 (2021).
36. E. L. Yarosz, C. H. Chang, The role of reactive oxygen species in regulating T cell-mediated immunity and disease. *Immune Netw.* **18**, e14 (2018).
37. S. H. Jackson, S. Devadas, J. Kwon, L. A. Pinto, M. S. Williams, T cells express a phagocyte-type NADPH oxidase that is activated after T cell receptor stimulation. *Nat. Immunol.* **5**, 818–827 (2004).
38. L. Ji *et al.*, N-acetylcysteine attenuates phosgene-induced acute lung injury via up-regulation of Nrf2 expression. *Inhal. Toxicol.* **22**, 535–542 (2010).
39. L. Zhang, Z. Zhu, J. Liu, Z. Zhu, Z. Hu, Protective effect of N-acetylcysteine (NAC) on renal ischemia/reperfusion injury through Nrf2 signaling pathway. *J. Recep. Signal. Transduct. Res.* **34**, 396–400 (2014).
40. T. Rangasamy *et al.*, Disruption of Nrf2 enhances susceptibility to severe airway inflammation and asthma in mice. *J. Exp. Med.* **202**, 47–59 (2005).
41. R. Nagashima *et al.*, Nrf2 suppresses allergic lung inflammation by attenuating the Type 2 innate lymphoid cell response. *J. Immunol.* **202**, 1331–1339 (2019).
42. C. A. Tibbitt *et al.*, Single-cell RNA sequencing of the T helper cell response to house dust mites defines a distinct gene expression signature in airway Th2 cells. *Immunity* **51**, 169–184.e165 (2019).
43. H. Y. Cho *et al.*, Nrf2-regulated PPARgamma expression is critical to protection against acute lung injury in mice. *Am. J. Respir. Crit. Care Med.* **182**, 170–182 (2010).
44. S. M. Ruppert *et al.*, JunD/AP-1-mediated gene expression promotes lymphocyte growth dependent on interleukin-7 signal transduction. *PLoS ONE* **7**, e32262 (2012).
45. J. F. Reichard, D. R. Petersen, Hepatic stellate cells lack AP-1 responsiveness to electrophiles and phorbol 12-myristate-13-acetate. *Biochem. Biophys. Res. Commun.* **322**, 842–853 (2004).
46. Y. Choi, H. Jeon, J. W. Akin, T. E. Curry, M. Jo, The FOS/AP-1 regulates metabolic changes and cholesterol synthesis in human periovulatory granulosa cells. *Endocrinology* **162**, bqab127 (2021).
47. Y. Endo, K. Hirahara, R. Yagi, D. J. Tumes, T. Nakayama, Pathogenic memory type Th2 cells in allergic inflammation. *Trends Immunol.* **35**, 69–78 (2014).
48. T. Nakajima *et al.*, ACC1-expressing pathogenic T helper 2 cell populations facilitate lung and skin inflammation in mice. *J. Exp. Med.* **218**, e20210639 (2021).
49. T. Y. Halim *et al.*, Group 2 innate lymphoid cells are critical for the initiation of adaptive T helper 2 cell-mediated allergic lung inflammation. *Immunity* **40**, 425–435 (2014).
50. T. Chen *et al.*, PPAR-gamma promotes type 2 immune responses in allergy and nematode infection. *Sci. Immunol.* **2**, eaal5196 (2017).
51. S. P. Nobs *et al.*, PPARgamma in dendritic cells and T cells drives pathogenic type-2 effector responses in lung inflammation. *J. Exp. Med.* **214**, 3015–3035 (2017).
52. N. S. Akins, T. C. Nielson, H. V. Le, Inhibition of glycolysis and glutaminolysis: An emerging drug discovery approach to combat cancer. *Curr. Top. Med. Chem.* **18**, 494–504 (2018).
53. F. Pouremamali, A. Pouremamali, M. Dadashpour, N. Soozangar, F. Jeddi, An update of Nrf2 activators and inhibitors in cancer prevention/promotion. *Cell Commun. Signal.* **20**, 100 (2022).
54. G. Choi *et al.*, NRF2 is a spatiotemporal metabolic hub driving the polyfunctionality of Th2 cells in allergic asthma. Gene Expression Omnibus. https://www.ncbi.nlm.nih.gov/geo/query/acc.cgi?acc=GSE241355. Deposited 21 August 2023.
55. G. Choi *et al.*, NRF2 is a spatiotemporal metabolic hub driving the polyfunctionality of Th2 cells in allergic asthma. Gene Expression Omnibus. https://www.ncbi.nlm.nih.gov/geo/query/acc.cgi?acc=GSE241138. Deposited 18 August 2023.